NSTAR 2026

Constraining the low-energy $S = -2$ meson-bayon interaction with two-particle correlations

Albert Feijoo

Institut de Física Corpuscular (IFIC), València

Collaborators:
V. Mantovani-Sarti (TUM), I. Vidaña (INFN Catania), J. Nieves (IFIC), A. Ramos (UB), T. Hyodo (OU), F. Giacosa (JKU) and Y. Kamiya (TU)

Motivation: Ξ^* spectrum

INSTITUT DE FÍSICA CORPUSCULAR

The nature and properties of doubly strange hyperons remain a subject of considerable controversy.

12 Ξ hyperons in the Particle Data Group:

- only the ground-state members of the SU(3) octet and decuplet have a four-star rating
- Ξ(1690), Ξ(1820), Ξ(1950) and Ξ(2030) received three-star status, yet only Ξ(1820) with well determined $J^P=3/2^-$ (evidence of a $J^P=1/2^-$ for Ξ(1690) from $\Lambda_c \to \Xi^-\pi^+K^+$)

  B. Aubert et al., Phys Rev D 78 (2008) 034008
- The rest, including Ξ(1620) resonance, are very poorly known (one or two-star status)

  The masses of the lightest resonances are close to several meson-baryon pair thresholds
  → plausible dominant molecular nature

  As clear example:

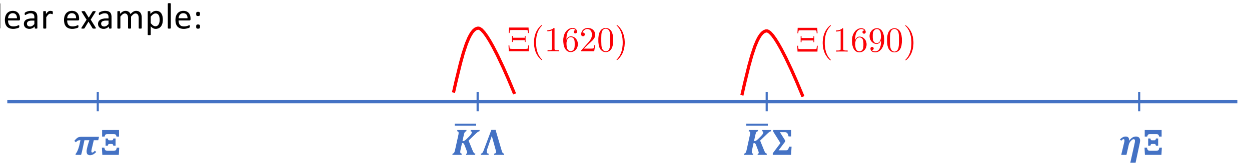

Motivation: Ξ(1620) and Ξ(1690) molecular nature

The molecular-nature conjecture for the ***Ξ(1620) and Ξ(1690)*** is further supported by:

- Unexpectedly small branching ratio ($M_{\Xi\pi} < M_{\bar{K}\Sigma}$→ larger phase space to decay in $\Xi\pi$)

PDG, Phys. Rev. D110, 030001 (2024)

$$\frac{\Gamma[\Xi(1690) \to \Xi\pi]}{\Gamma[\Xi(1690) \to \Sigma\bar{K}]} < 0.09$$

Complex internal structure (beyond ordinary 3-quark baryon)

UChPT-based study explained this value: *Ξ(1690) dynamically generated* $\bar{K}\Sigma$ quasibound state with nearly vanishing coupling to $\pi\Xi$ channel

T. Sekihara, PTEP 2015 (2015) 9, 091D01

- The problem have been formulated in terms of a Unitary extension of ChPT in coupled channels by many groups

→ some describe just one of the states properly, others can describe both states simultaneously yet only qualitatively

A. Ramos, E. Oset, C. Bennhold, PRL 89 (2002) 252001
C. Garcia-Recio, M.F.M. Lutz, J. Nieves, PLB 582 (2004) 49–54
D. Gamermann, C. Garcia-Recio, J. Nieves, et al., PRD 84 (2011) 056017
K.P. Khemchandani, A. Martínez Torres, A. Hosaka, et al., PRD 97, 034005 (2018)
T. Nishibuchi, T. Hyodo, PRC 109 (2024) 1, 015203

Different levels of sophistication in approaches:
WT-like contact term in UChPT scheme or in SU(6) extension of the Chiral Lagrangian…
Inclusion of t-, s- and u-channel diagrams

Common main ingredients:
Leading-order s-wave contact term, interaction between pseudoscalar octet ⊕ ground-state baryon octet

Motivation: Effects of the NLO terms on the Ξ^* spectrum

A.F., V. Valcarce, V. Magas, Phys. Lett. B 841 (2023) 137927

Incorporation of higher order corrections (Born + NLO terms) in the Lagrangian can modify the interplay between coupled channels thereby modifying the pole locations and widths

$$\mathcal{L}^{eff}(B,U) = \mathcal{L}^{(1)}_{MB}(B,U) + \mathcal{L}^{(2)}_{MB}(B,U)$$

$$\mathcal{L}^{(1)}_{MB} = \langle \bar{B}(i\gamma_\mu D^\mu - M_0)B\rangle + \frac{1}{2}D\langle \bar{B}\gamma_\mu\gamma_5\{u^\mu, B\}\rangle + \frac{1}{2}F\langle \bar{B}\gamma_\mu\gamma_5[u^\mu, B]\rangle$$

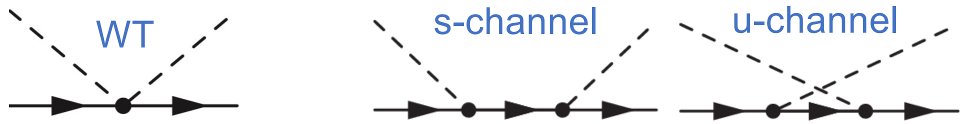

Born terms

NLO contact terms

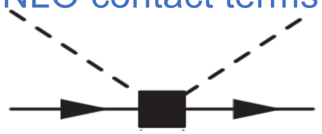

$$\mathcal{L}^{(2)}_{MB} = b_D\langle \bar{B}\{\chi_+, B\}\rangle + b_F\langle \bar{B}[\chi_+, B]\rangle + b_0\langle \bar{B}B\rangle\langle\chi_+\rangle + d_1\langle \bar{B}\{u_\mu, [u^\mu, B]\}\rangle$$
$$+ d_2\langle \bar{B}[u_\mu, [u^\mu, B]]\rangle + d_3\langle \bar{B}u_\mu\rangle\langle u^\mu B\rangle + d_4\langle \bar{B}B\rangle\langle u^\mu u_\mu\rangle$$

$\boldsymbol{b_0, b_D, b_F, d_1, d_2, d_3, d_4}$ LECs are not established by the underlying theory

No available scattering data to fix the LECs → SU(3) symmetry is assumed and LECs taken from BCN model (same approach constrained by the S=-1 meson-baryon scattering data)

A.F., V. Magas and A. Ramos, Phys. Rev. C 99, no.3, 035211 (2019)

Motivation: Effects of the NLO terms on the Ξ^* spectrum

The presence of the Ξ(1620) and Ξ(1690) requires a non-perturbative
→ solve the Bethe–Salpeter equation in coupled channels with on-shell factorization

$$T = (1 - VG)^{-1} V \longrightarrow T_{ij}$$

$$G_l = \frac{2M_l}{(4\pi)^2}\left\{a_l(\mu) + \ln\frac{M_l^2}{\mu^2} + \frac{m_l^2 - M_l^2 + s}{2s}\ln\frac{m_l^2}{M_l^2} + \frac{q_{\rm cm}}{\sqrt{s}}\ln\left[\frac{(s+2\sqrt{s}q_{\rm cm})^2-(M_l^2-m_l^2)^2}{(s-2\sqrt{s}q_{\rm cm})^2-(M_l^2-m_l^2)^2}\right]\right\}$$

subtraction constants (SCs) for the dimensional regularization scale $\mu = 630 MeV$ in all the "l" channels

isospin symmetry

$$a_{\pi^0\Xi^0} = a_{\pi^+\Xi^-} = a_{\pi\Xi}$$

$$a_{\bar{K}^0\Lambda} = a_{\bar{K}\Lambda}$$

$$a_{\bar{K}^0\Sigma^0} = a_{K^-\Sigma^+} = a_{\bar{K}\Sigma}$$

$$a_{\eta\Xi^0} = a_{\eta\Xi}$$

SCs are unknown parameters to be fitted to the experiment ($a_l \sim -2$)
→ Tunned to reproduce the experimental masses and widths of the Ξ(1620) and Ξ(1690):

Belle Coll., Phys Rev. Lett. 122, 072501 (2019)

$$M_{\Xi(1620)} = 1610.4 \pm 6.0(\text{stat})^{+6.1}_{-4.2}(\text{syst})$$

$$\Gamma_{\Xi(1620)} = 59.9 \pm 4.8(\text{stat})^{+2.8}_{-7.1}(\text{syst})$$

LHCb Coll., Science Bulletin 66 (2021) 1278–1287

$$M_{\Xi(1690)} = 1692.0 \pm 1.3^{+1.2}_{-0.4}\,\text{MeV}$$

$$\Gamma_{\Xi(1690)} = 25.9 \pm 9.5^{+14.0}_{-13.5}\,\text{MeV}$$

Motivation: Effects of the NLO terms on the Ξ^* spectrum

A.F., V. Valcarce, V. Magas, PLB 841 (2023) 137927, PLB 853 (2024) 138660 (erratum)

Pole content:

BCN Model	$\Xi(1620)$		$\Xi(1690)$	
M [MeV]	1606.86		1680.99	
Γ [MeV]	171.18		5.17	
	g_i	$\lvert g_i\rvert$	g_i	$\lvert g_i\rvert$
$\pi^+\Xi^-$	$1.71 + i\,0.83$	1.90	$-0.17 + i\,0.07$	0.19
$\pi^0\Xi^0$	$-1.21 - i\,0.59$	1.35	$0.16 - i\,0.04$	0.16
$\bar{K}^0\Lambda$	$-1.95 - i\,0.21$	1.96	$-0.48 - i\,0.06$	0.49
$K^-\Sigma^+$	$0.76 - i\,0.11$	0.77	$-1.43 + i\,0.11$	1.44
$\bar{K}^0\Sigma^0$	$-0.54 + i\,0.07$	0.55	$1.05 - i\,0.07$	1.05
$\eta\Xi^0$	$-0.05 + i\,0.10$	0.12	$0.74 - i\,0.05$	0.74

Belle: $M = 1610.4 \pm 6.0^{+5.9}_{-3.5}$ MeV, $\Gamma = 59.9 \pm 4.8^{+2.8}_{-3.0}$ MeV

LHCb: $M = 1692.0 \pm 1.3^{+1.2}_{-0.4}$ MeV, $\Gamma = 25.9 \pm 9.5^{+14.0}_{-13.5}$ MeV

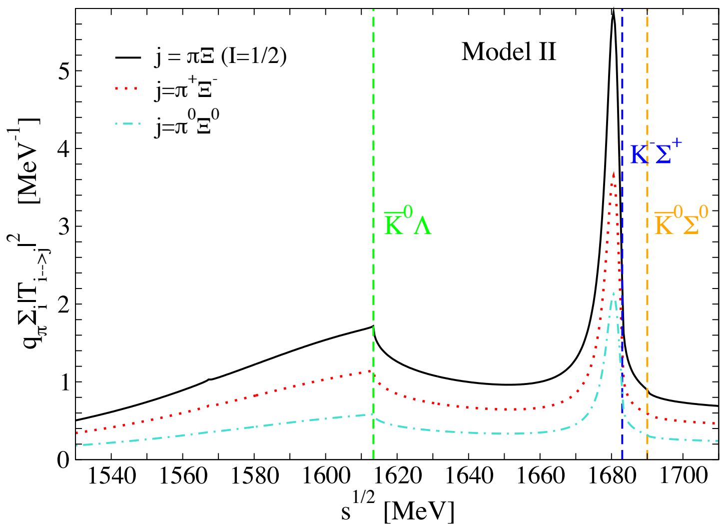

→ First simultaneous generation of both poles with reasonable reproduction of masses and widths

→ The Flatté effect experienced by the Ξ(1620) signal at the $\bar{K}^0\Lambda$ threshold fixes the incompatibility between the experimental and the theoretical values living an apparent width ~75MeV

→ Coupling pattern consistent with previous works

Impact of the Femtoscopic data on Ξ^* spectrum

Weak decays of heavy hadrons are **Key inputs** for hadron spectroscopy

- Full theoretical control is **hard** → many decay mechanisms involved
- Known hierarchy: external emission > internal emission > *W*-exchange > annihilation

→But **relative weights** in each decay mechanisms are generally **unknown**.

Hadron femtoscopy

- Now a **powerful tool** to constrain hadron interactions where scattering data are unavailable.
- The **Koonin–Pratt formalism** to calculate CFs provides a clean, controlled framework, giving tighter **constraints** (despite inherent offshell ambiguities in the scattering wave function)

Testing the BCN model with femtoscopy

- ALICE collaboration released the $K^-\Lambda$ CF analysis in 2023 Phys. Lett. B 845 (2023) 138145
- The validity of the BCN model (NLO) was confronted using femto data via the KPF
- The resulting theoretical $K^-\Lambda$ CF failed to describe the data—not even the trend
- Then the model parameters (LECs and SCs) fitted to the femto data, aiming to shed light on the *nature of the Ξ^* states*

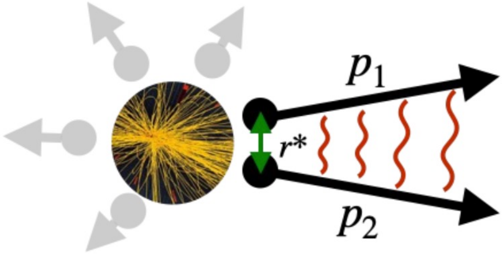

The CF in multi-channel systems for a given pair "*i*" can be express *within the KP formalism* as:

$$C_i(k^*) = \sum_j \omega_j^{\mathrm{prod.}} \int d^3r^* S_j(r^*) |\psi_{ji}(k^*, r^*)|^2$$

Channel j	ω_j^{prod}
$K^-\Lambda$	1.000
$\pi^-\Xi^0$	$1.536^{+0.005}_{-0.012}$
$\pi^0\Xi^-$	$1.584^{+0.001}_{-0.006}$
$K^-\Sigma^0$	$0.682^{+0.001}_{-0.001}$
$\overline{K}^0\Sigma^-$	$0.630^{+0.001}_{-0.004}$
$\eta\Xi^-$	$0.178^{+0.023}_{-0.022}$

$\boldsymbol{\omega_j^{prod}}$: production weights take into account the initially produced *j* pairs that can convert to the measured *i* final state

- ✓ Depend on yields & kinematics: $\boldsymbol{\omega_j^{prod}} = \frac{N_j^{prim}}{N_i^{prim}} = \frac{N_{j_A}^{prim} N_{j_B}^{prim}}{N_{i_A}^{prim} N_{i_B}^{prim}}$
- ✓ Particle abundances estimated from **Thermal**[1] & Transport[2] models

Impact of the Femtoscopic data on Ξ^* spectrum: Koonin-Pratt formalism

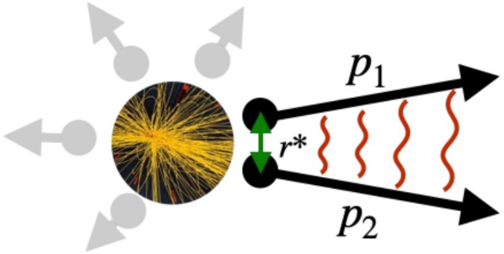

The CF in multi-channel systems for a given pair "*i*" can be express *within the KP formalism* as:

$$C_i(k^*) = \sum_j \omega_j^{\text{prod.}} \int d^3r^* S_j(r^*) |\psi_{ji}(k^*, r^*)|^2$$

$S_j(r^*)$: emitting source describes the probability of emitting the particle pair *j* at a relative distance r^*.
For the present cases, it is taken to be:

$$S_j(r^*) = \Lambda_s \Big(\omega\, G_1(r^*) + (1-\omega)\, G_2(r^*)\Big)$$

$$G_i(r^*) = \frac{1}{\sqrt{4\pi} R_i^3} \exp\left(-\frac{r^{*2}}{4R_i^2}\right), \quad (i = 1, 2)$$

Channels	R_1 (fm)	R_2 (fm)	ω	Λ_s
$K^-\Lambda$, $\Sigma\bar{K}$	$1.202^{+0.043}_{-0.042}$	$2.330^{+0.050}_{-0.045}$	$0.7993^{+0.0037}_{-0.0027}$	$0.9806^{+0.0006}_{-0.0008}$
$\pi\Xi$	$1.371^{+0.041}_{-0.040}$	$3.338^{+0.038}_{-0.035}$	$0.7415^{+0.0017}_{-0.0035}$	$0.9806^{+0.0019}_{-0.0013}$
$\eta\Xi^-$	$1.21^{+0.040}_{-0.040}$	$2.28^{+0.040}_{-0.040}$	0.86	$0.988^{+0.001}_{-0.001}$

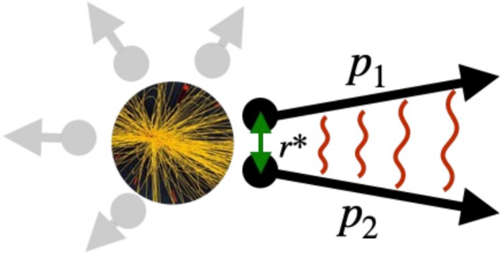

The CF in multi-channel systems for a given pair "*i*" can be express *within the KP formalism* as:

$$C_i(k^*) = \sum_j \omega_j^{\text{prod.}} \int d^3r^* S_j(r^*) |\psi_{ji}(k^*, r^*)|^2$$

$\Psi_{ji}(k^*, r^*)$: relative wave function describes the transition from a given initial channel *j* to the final observed channel *i,* it can be obtained from the scattering amplitude T_{ji} as

$$\psi_{ji}(p,r) = \delta_{ji} j_0(pr) + \int \frac{d^3q}{(2\pi)^3} \frac{1}{2\omega_j(q)} \frac{M_j}{E_j(q)} \frac{T_{ji}(\sqrt{s}, p, q)\ j_0(qr)}{\sqrt{s} - \omega_j(q) - E_j(q) + i\epsilon}$$

Impact of the Femtoscopic data on Ξ^* spectrum: Results

V. Mantovani Sarti, A.F., I. Vidaña, et al, Phys. Rev. D 110 (2024) 1, L011505

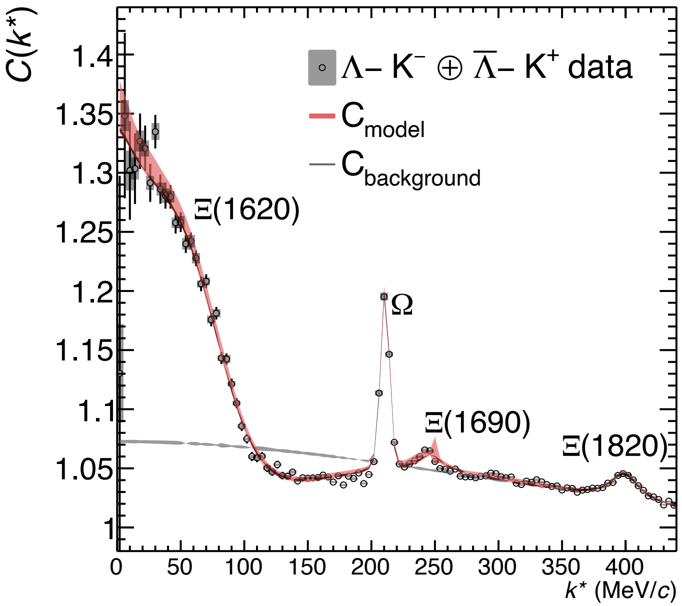

$$C(k^*) = N_D \times C_{\rm model}(k^*) \times C_{\rm background}(k^*)$$

$$C_{\rm model}(k^*) = 1 + \lambda_{\rm gen} \times (C_{\rm gen}(k^*) - 1)$$

$$+ \sum_{\rm res} \lambda_{\rm res} \times (C_{\rm res}(k^*) - 1)$$

Pole content with the determined scattering amplitudes:

mass M:	1612.68 MeV		1670.28 MeV	
width Γ:	24.57 MeV		7.44 MeV	
Riemann sheet:	$(- - - + ++)$		$(- - - + ++)$	
	$\lvert g_i \rvert$	$\lvert g_i^2 dG/dE \rvert$	$\lvert g_i \rvert$	$\lvert g_i^2 dG/dE \rvert$
$\pi^-\Xi^0(1454)$	0.51	0.014	0.22	0.002
$\pi^0\Xi^-(1456)$	0.36	0.007	0.39	0.007
$\Lambda K^-(1609)$	0.94	0.162	0.07	0.000
$K^-\Sigma^0(1686)$	0.17	0.002	2.20	0.761
$\bar{K}^0\Sigma^-(1695)$	0.21	0.003	1.37	0.230
$\eta\Xi^-(1868)$	5.86	0.937	0.05	0.000
Experimental Ξ^*:	$\Xi(1620)$ BELLE		$\Xi(1690)$ PDG	
mass M:	$1610.4 \pm 6.0^{+5.9}_{-3.5}$ MeV		1690 ± 10 MeV	
width Γ:	$59.9 \pm 4.8^{+2.8}_{-3.0}$ MeV		20 ± 15 MeV	

→ Both poles found in the physically relevant RS
→ Pole masses and widths compatible with experimental data
→ Novel aspect: g_i show a different pattern for the Ξ(1620)

- Former works interpret it as a $\pi\Xi - \bar{K}\Lambda$ molecule (+ non-negligible $\bar{K}\Sigma$ coupling)
- In this study, Ξ(1620) is a molecule basically consisting of $K^-\Lambda - \eta\Xi$ mixing

Compatibility study between $K^-\Lambda$ CF and $K^-\Lambda$ IMD from $\Xi_b^- \to J/\psi K^-\Lambda$

The scattering amplitudes constrained using Femtoscopic data shed novel coupling-pattern paradigm for the Ξ(1620) molecular state
→ It is mandatory to check the realistic character of this interpretation

Why test the model in the $K^-\Lambda$ spectrum?

- In the CF analysis, the scattering information enters through the coupled–channel amplitudes $t_{i\to K^-\Lambda}$, filtered by the **source functions** and weighted by the **production coefficients** (primary p-p collision)
  → CF mainly probes the **final-state interaction** under a **specific production mechanism**

- In $\Xi_b^- \to J/\psi K^-\Lambda$ decay, the relevant amplitudes are the **same** $t_{i\to K^-\Lambda}$, but they appear multiplied by **different production weights** determined by the weak decay dynamics
  → The decay emphasizes **different channel contributions** compared with CF

- Each mechanism provide different sensitivity to the pole structure of Ξ(1620) and Ξ(1690)

→ **Testing LHCb spectra** (Science Bulletin 66 (2021) 1278–1287) **assesses whether the amplitudes constrained in CF remain consistent once a different production mechanism is at play.**

Compatibility study between $K^-\Lambda$ CF and $K^-\Lambda$ IMD from $\Xi_b^- \to J/\psi K^-\Lambda$

Internal emission process and hadronization mechanism

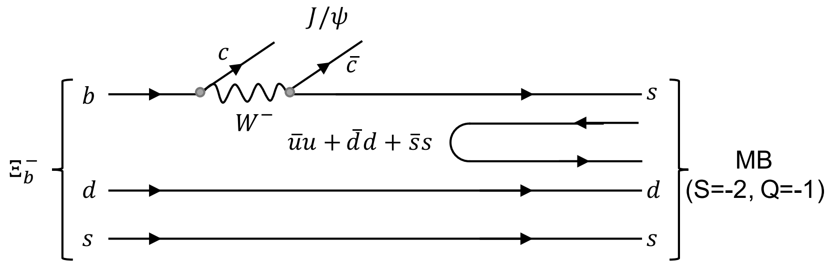

$$|\Xi_b^-\rangle = |b(ds - sd)\rangle / \sqrt{2} \to \bar{c}c\, |s(\bar{u}u + \bar{d}d + \bar{s}s)(ds - sd)\rangle / \sqrt{2} = |J/\psi\rangle\, |H\rangle$$

$$|H\rangle = \frac{1}{\sqrt{2}} |s(\bar{u}u + \bar{d}d + \bar{s}s)(ds - sd)\rangle = \frac{1}{\sqrt{2}} \sum_{i=1}^{3} \phi_{3i}\, q_i (ds - sd) =$$

$$= \frac{1}{\sqrt{2}} K^-\Sigma^0 + \bar{K}^0\Sigma^- - \frac{1}{\sqrt{6}} K^-\Lambda - \frac{1}{\sqrt{3}} \eta\Xi^-$$

Production weights

$\boxed{h_{K^-\Sigma^0} = \frac{1}{\sqrt{2}}}$ $\boxed{h_{\bar{K}^0\Sigma^-} = 1}$ $\boxed{h_{K^-\Lambda} = -\frac{1}{\sqrt{6}}}$ $\boxed{h_{\eta\Xi^-} = -\frac{1}{\sqrt{3}}}$ $\boxed{h_{\pi^-\Xi^0} = h_{\pi^0\Xi^-} = 0}$

Diagrams accounted for to calculate the amplitude of the process:

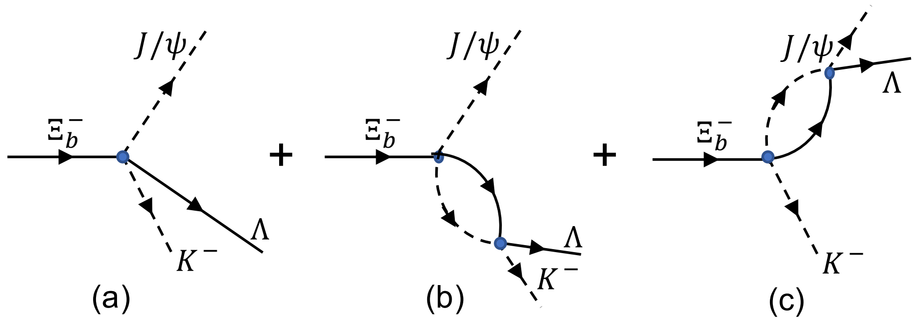

a) Tree level diagram contributing to background
b) (S=-1) MB FSI (Chiral Lagrangian up to NLO): BCN (Phys. Lett. B 841 (2023) 137927) and VBC (Phys. Rev. D 110 (2024) 1, L011505) models
c) J/ψΛ FSI (HQSS and HG formalism)
A.F., W.F. Wang, C. W. Xiao et al., Phys.Lett.B 839 (2023) 137760

Compatibility study between $K^-\Lambda$ CF and $K^-\Lambda$ IMD from $\Xi_b^- \to J/\psi K^-\Lambda$

INSTITUT DE FÍSICA CORPUSCULAR

The decay amplitude should preserve the total spin $J(\Xi_b^-) = 1/2$

$$J(J/\psi) = 1,\ \ J(\Lambda) = 1/2\ (\text{s-wave}) \to J(J/\psi\Lambda) = 1/2,\, 3/2$$

$$J(K^-) = 0$$

Depending on the total spin of the $J/\psi\Lambda$ system (1/2 or 3/2), one should take the corresponding relative angular momentum (L=0 or 1) of the K^- with respect to the $J/\psi\Lambda$

Amplitude of the decay process (with the spin considerations)

$$|\mathcal{M}|^2 = \mathcal{N}\left[3V_p^2\left|T_{1/2}^{\text{s}-\text{wave}}\right|^2 + \frac{3}{2}\vec{q}^{\,2}B^2\left|T_{3/2}^{\text{p}-\text{wave}}\right|^2 + 3\vec{q}^{\,2}B'^2\left|T_{1/2}^{\text{p}-\text{wave}}\right|^2 + \sum_i |t_{\Xi_i^*}^{BW}(m_{K^-\Lambda})|^2\right]$$

$$\boxed{T^L_{J_{J/\psi\Lambda}}}$$

Coherent sum of the Feynman diagrams with relative angular momentum L and total $J/\psi\Lambda$ spin

H.-X. Chen, L.-S. Geng, W.-H. Liang,et al., Phys. Rev. C 93, 065203 (2016)

Compatibility study between $K^-\Lambda$ CF and $K^-\Lambda$ IMD from $\Xi_b^- \to J/\psi K^-\Lambda$

IFIC INSTITUT DE FÍSICA CORPUSCULAR

Amplitude of the decay process

$$|\mathcal{M}|^2 = \mathcal{N}\Big[3V_p^2\left|T_{1/2}^{\mathrm{s-wave}}\right|^2 + \frac{3}{2}\vec{q}^2 B^2\left|T_{3/2}^{\mathrm{p-wave}}\right|^2 + 3\vec{q}^2 B'^2\left|T_{1/2}^{\mathrm{p-wave}}\right|^2 + \boxed{\sum_i |t_{\Xi_i^*}^{BW}(m_{K^-\Lambda})|^2\Big]}$$

V_P, B and B' encode the weak processes for L=0,1

→ smooth behavior in this energy window, assumed constant

→ $V_p \sim 1$ (dominant K^- in s-wave), $B \approx B'$ (10% relative to V_P)

→ Maximum $q_{K^-} \approx 1000 MeV/c$, then $B = B' = 10^{-4}$

The global normalization N factor will absorb the strength of the weak process

→ Extracted from the ratio between the integrated theoretical $K^-\Lambda$ invariant mass distribution over the experimental one in [1680,2700] MeV (ensures direct comparison to data)

Resonances appearing in the $K^-\Lambda$ IMD not generated by the model (pseudoscalar-baryon (1/2⁺) limited to s-wave)
$i = \Xi(1820), \Xi(1950), \Xi(2030)$

$\Gamma(\bar{K}\Lambda)/\Gamma_{\mathrm{total}} = 0.25$ PDG+LHCb measurement

$\Gamma_{\mathrm{total}} = 8\, MeV$

$$t_{\Xi(1820)}^{BW}(m_{\Lambda K^-}) = \frac{g_{\Lambda K^-}^2}{m_{\Lambda K^-} - M_{\Xi(1820)} + i\frac{\Gamma_{\Xi(1820)}}{2}}$$

The contributions from $\Xi(1950)$ and $\Xi(2030)$ states obtained employing an ordinary relativistic Breit-Wigner (masses and widths are taken from LHCb measurement)

LHCb Coll., Science Bulletin 66 (2021) 1278–1287

Compatibility study between $K^-\Lambda$ CF and $K^-\Lambda$ IMD from $\Xi_b^- \to J/\psi K^-\Lambda$

Scenario A

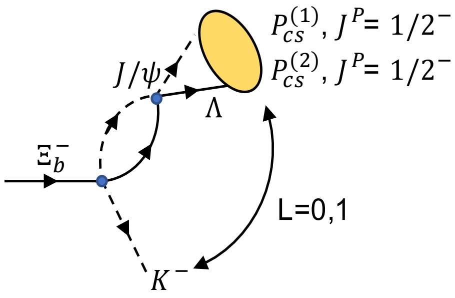

$$T_{1/2}^{\text{s-wave}} = h_{\Lambda K^-} + h_{\Lambda K^-} G_{J/\psi\Lambda}(m_{J/\psi\Lambda}) t_{J/\psi\Lambda, J/\psi\Lambda}(m_{J/\psi\Lambda}) + \sum_i h_i G_i(m_{K^-\Lambda}) t_{i,K^-\Lambda}(m_{K^-\Lambda})$$

$$T_{3/2}^{\text{p-wave}} = h_{\Lambda K^-}$$

$$T_{1/2}^{\text{p-wave}} = h_{\Lambda K^-} + + h_{\Lambda K^-} G_{J/\psi\Lambda}(m_{J/\psi\Lambda})\, t_{J/\psi\Lambda, J/\psi\Lambda}(m_{J/\psi\Lambda})$$

Scenario B

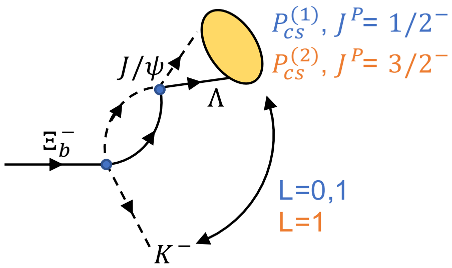

$$T_{1/2}^{\text{s-wave}} = h_{K^-\Lambda} + h_{K^-\Lambda} G_{J/\psi\Lambda}(m_{J/\psi\Lambda}) t^{BW}_{P_{cs}^{(1)}}(m_{J/\psi\Lambda}) + \sum_i h_i G_i(m_{K^-\Lambda}) t_{i,K^-\Lambda}(m_{K^-\Lambda})$$

$$T_{3/2}^{\text{p-wave}} = h_{K^-\Lambda} + h_{K^-\Lambda} G_{J/\psi\Lambda}(m_{J/\psi\Lambda})\, t^{BW}_{P_{cs}^{(2)}}(m_{J/\psi\Lambda})$$

$$T_{1/2}^{\text{p-wave}} = h_{K^-\Lambda} + h_{K^-\Lambda} G_{J/\psi\Lambda}(m_{J/\psi\Lambda}) t^{BW}_{P_{cs}^{(1)}}(m_{J/\psi\Lambda})$$

Compatibility study between $K^-\Lambda$ CF and $K^-\Lambda$ IMD from $\Xi_b^- \to J/\psi K^-\Lambda$

Scenario C

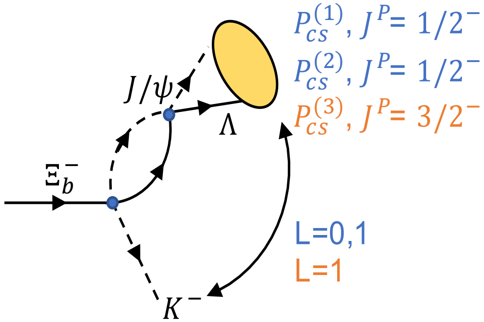

$$T_{1/2}^{\mathrm{s-wave}} = h_{K^-\Lambda} + h_{K^-\Lambda} G_{J/\psi\Lambda}(m_{J/\psi\Lambda}) t_{J/\psi\Lambda, J/\psi\Lambda}(m_{J/\psi\Lambda})$$
$$+ \sum_i h_i G_i(m_{K^-\Lambda}) t_{i,K^-\Lambda}(m_{K^-\Lambda})$$

$$T_{3/2}^{\mathrm{p-wave}} = h_{K^-\Lambda} + h_{K^-\Lambda} G_{J/\psi\Lambda}(m_{J/\psi\Lambda}) t^{BW}_{P_{cs}^{(3)}}(m_{J/\psi\Lambda})$$

$$T_{1/2}^{\mathrm{p-wave}} = h_{K^-\Lambda} + h_{K^-\Lambda} G_{J/\psi\Lambda}(m_{J/\psi\Lambda})\, t_{J/\psi\Lambda, J/\psi\Lambda}(m_{J/\psi\Lambda})$$

A.F., V. Mantovani Sarti, J. Nieves, A. Ramos and I. Vidaña. Phys. Rev. D 111 (2025) 1, 014022

Compatibility study between $K^-\Lambda$ CF and $K^-\Lambda$ IMD from $\Xi_b^- \to J/\psi K^-\Lambda$

Dalitz plot:

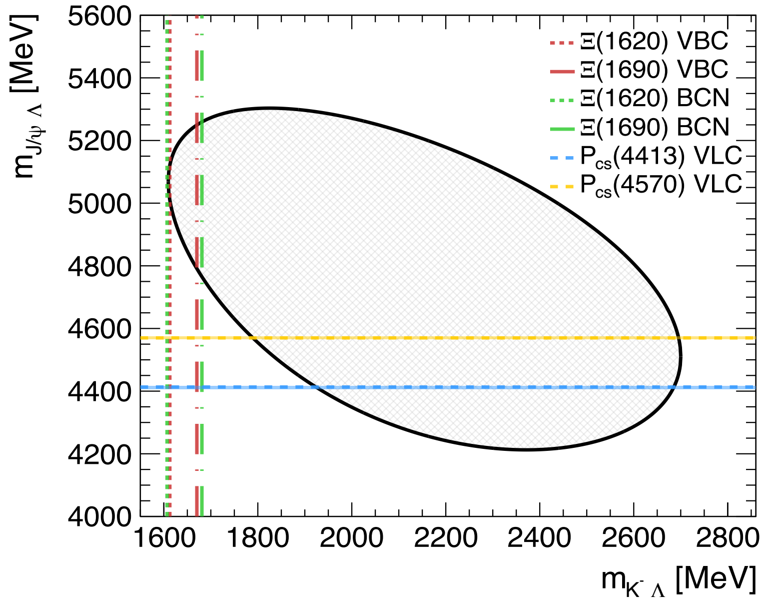

The poles dynamically generated by the $t_{J/\psi\Lambda}$ start to influence the $d\Gamma/dm^2_{K^-\Lambda}$ distribution from around 1800 MeV onward

Double differential cross-section for the $\Xi_b^- \to J/\psi K^-\Lambda$ decay process:

$$\frac{d^2\Gamma}{dm^2_{K^-\Lambda}dm^2_{J/\psi\Lambda}} = \frac{M_{\Xi_b}M_\Lambda}{64\pi^3 M^3_{\Xi_b}}|\mathcal{M}(m_{K^-\Lambda}, m_{J/\psi\Lambda})|^2$$

$d\Gamma/dm^2_{K^-\Lambda}$ requires fixing $m_{K^-\Lambda}$ invariant mass and integrate over $m_{J/\psi\Lambda}$:

$$(m^2_{J/\psi\Lambda})_{\max} = (E^*_\Lambda + E^*_{J/\psi})^2 - \left(\sqrt{E^{*\,2}_\Lambda - M^2_\Lambda} - \sqrt{E^{*2}_{J/\psi} - m^2_{J/\psi}}\right)^2$$

$$(m^2_{J/\psi\Lambda})_{\min} = (E^*_\Lambda + E^*_{J/\psi})^2 - \left(\sqrt{E^{*\,2}_\Lambda - M^2_\Lambda} + \sqrt{E^{*2}_{J/\psi} - m^2_{J/\psi}}\right)^2$$

$$E^*_\Lambda = \frac{m^2_{K^-\Lambda} - m^2_{K^-} + M^2_\Lambda}{2m_{K^-\Lambda}}\ , \quad E^*_{J/\psi} = \frac{M^2_{\Xi_b} - m^2_{K^-\Lambda} - m^2_{J/\psi}}{2m_{K^-\Lambda}}$$

A.F., V. Mantovani Sarti, J. Nieves, A. Ramos and I. Vidaña. Phys. Rev. D 111 (2025) 1, 014022

Compatibility study between $K^-\Lambda$ CF and $K^-\Lambda$ IMD from $\Xi_b^- \to J/\psi K^- \Lambda$

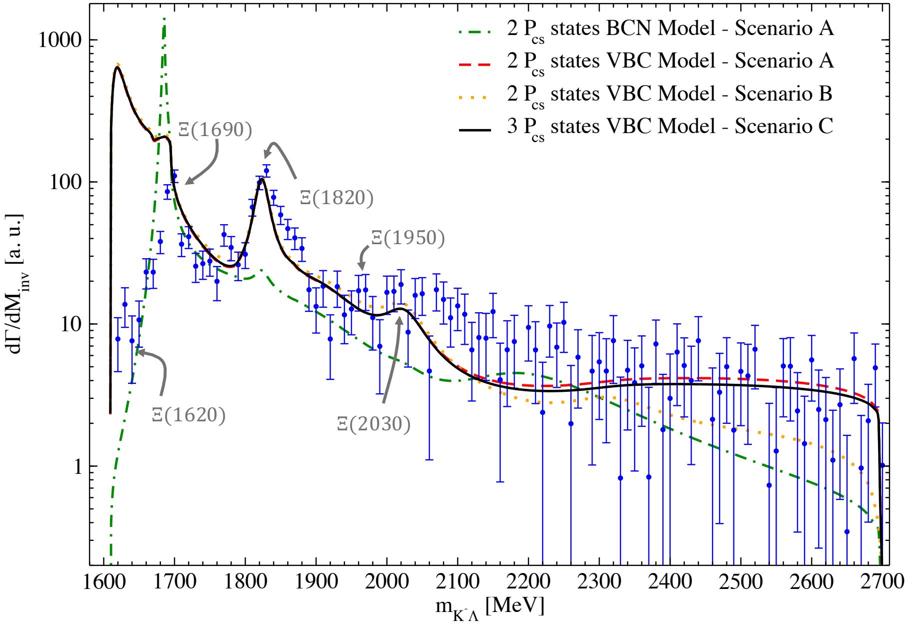

A.F., V. Mantovani Sarti, J. Nieves, A. Ramos and I. Vidaña, Phys. Rev. D 111 (2025) 1, 014022

This decay proceeds through the intermediate $i =$ $K^-\Lambda, \bar{K}^0\Sigma^-, K^-\Sigma^0, \eta\Xi^-$ channels via the $\boldsymbol{t_{i\to K^-\Lambda}}$

- VBC: generates $\Xi(1620)$ above $K^-\Lambda$ threshold coupling to $K^-\Lambda$ and $\eta\Xi^-$(strongly) → overshooting the LHCb data points
- BCN: generates $\Xi(1620)$ below $K^-\Lambda$ threshold (broad structure + Flatté effect) coupling to $K^-\Lambda$ and $\boldsymbol{\pi\Xi}$ channels (strongly) → suppressed peak structure in the IMD
- Both models overestimate the $\Xi(1690)$ experimental peak (VBC by a factor 2, BCN by an order of magnitude)
- The background generated by the VBC combined with the BWs is in good agreement with LHCb data from 1800 MeV onward
- All configurations of $\boldsymbol{P_{cs}}$ states in the $J/\psi\Lambda$ invariant mass provide a similar good description of the LHCb data (better for those configurations where the heavier one has J=3/2)

Compatibility study between $K^-\Lambda$ CF and $K^-\Lambda$ IMD from $\Xi_b^- \to J/\psi K^-\Lambda$

INSTITUT DE FÍSICA CORPUSCULAR

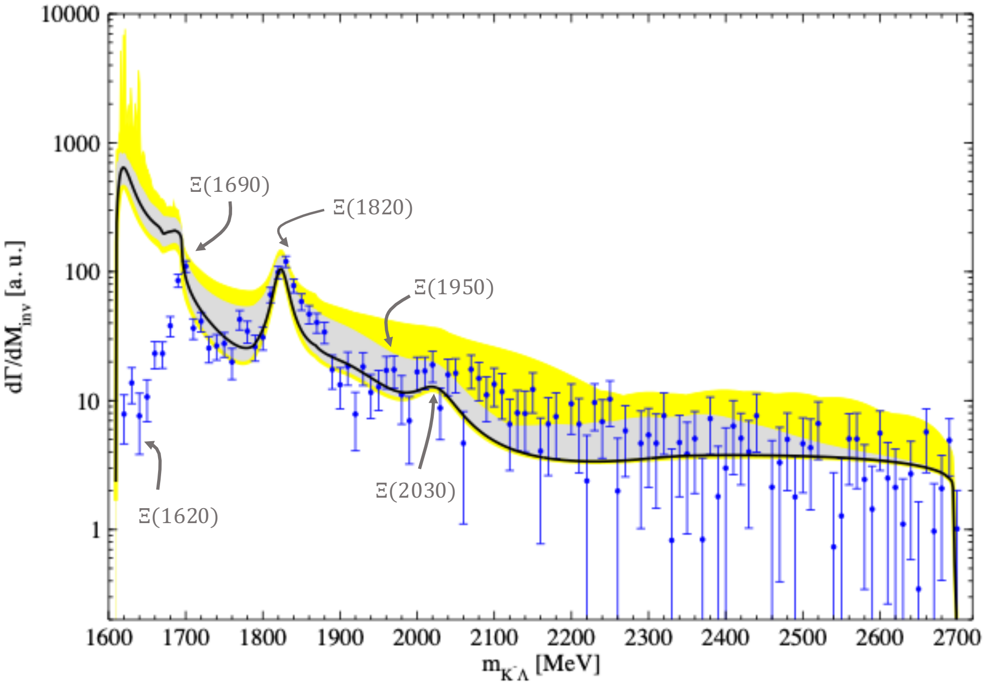

A.F., V. Mantovani Sarti, J. Nieves, A. Ramos and I. Vidaña, Phys. Rev. D 111 (2025) 1, 014022

Error bands for VBC model (scenario C) estimated from the uncertainties of the LECs and SCs (1σ grey band, 2σ yellow band)

- Error bands clearly show that experimental data fall within the $\Xi(1690)$ resonance region, while they highlight the inability of the model to properly describe the spectrum below 1690 MeV

→ NEED FOR ADDITIONAL EXPERIMENTAL DATA TO FURTHER CONSTRAIN AND REFINE THE MODELS

Recent study with same conclusions:
Veloso, Khemchandani et al., arXiv:2608.27736

CONCLUSIONS

First study connecting a **UχPT model at NLO (VBC),** constrained to **ALICE** $K^-\Lambda$ CF, with the **LHCb** $K^-\Lambda$ invariant–mass spectrum in $\Xi_b^- \to J/\psi K^-\Lambda$.

VBC model provides a **novel molecular interpretation** of the lowest Ξ^* states, consistent with present measurements, and different from previous S=−2 approaches.

Comparison between **BCN** and **VBC** UχPT models shows that **VBC gives a better description** of the measured $K^-\Lambda$ spectrum above the 1690 MeV region.

The $J/\psi\Lambda$ amplitude, built from HQSS and LHG with a unitary extension, dynamically generates **two degenerate $\boldsymbol{P_{cs}}$** states. Testing different $\boldsymbol{P_{cs}}$ spin–parity and multiplicities shows **very small impact** on the $K^-\Lambda$ spectrum.

Some tension between models and LHCb is visible near the $K^-\Lambda$ threshold, driven by the $\Xi(1620)$ and its model-dependent coupling. This highlights the importance of **precise constraints on the** $\Xi(1620)$ properties and its coupled channels. Additional experimental input on $\boldsymbol{\pi\Xi}$, $\boldsymbol{\bar{K}\Sigma}$ and $\boldsymbol{\eta\Xi}$ would significantly improve the determination of the UχPT parameters in the **S=−2** sector.
Future work: exploit new **ALICE** $\Xi^-\pi^+$ correlations and include the Belle $\Xi_c^+ \to \Xi^-\pi^+\pi^+$decay in this analysis.

Experimental background: Weak decays (Belle)

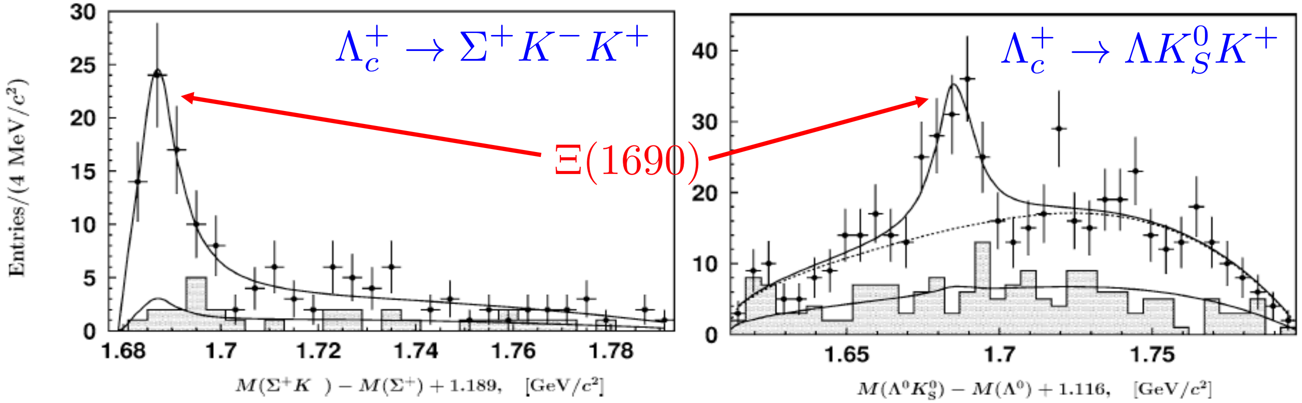

$\Lambda_c^+ \to \Xi(1690)^0 K^+$

Belle Coll., Phys Lett. B 524 (2002) 33–43

$$\frac{\mathcal{B}\,[\Lambda_c^+ \to \Xi(1960)^0 K^+ \to \Sigma^+ K^- K^+]}{\mathcal{B}\,[\Lambda_c^+ \to \Xi(1960)^0 K^+ \to \Lambda \bar{K}^0 K^+]}$$
$$= 0.62 \pm 0.33$$

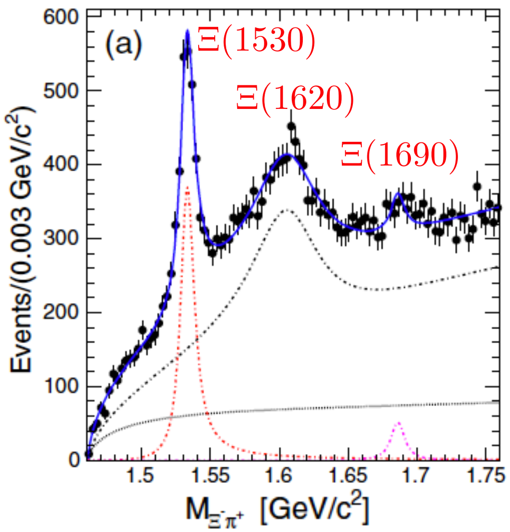

First observation of the $\Xi(1620)$ via $\Xi_c^+ \to \Xi^- \pi^+ \pi^+$

Belle Coll., Phys Rev. Lett. 122, 072501 (2019)

Clear evidences for $\Xi(1530)$, $\Xi(1620)$ and $\Xi(1690)$

Determination of the $\Xi(1620)$ properties:

$$M_{\Xi(1620)} = 1610.4 \pm 6.0(\text{stat})^{+6.1}_{-4.2}(\text{syst})$$

$$\Gamma_{\Xi(1620)} = 59.9 \pm 4.8(\text{stat})^{+2.8}_{-7.1}(\text{syst})$$

Experimental background: Weak decay (LHCb) and Femtoscopy (ALICE)

$\Xi_b^- \to J/\psi \Lambda K^-$

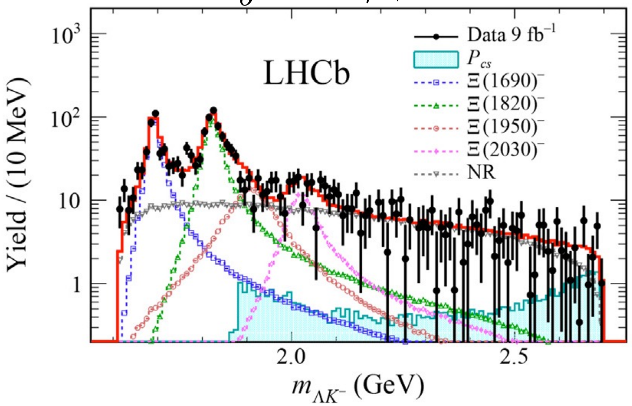

LHCb Coll., Science Bulletin 66 (2021) 1278–1287

Determination of the $\Xi(1690)$ and $\Xi(1820)$ properties:

$$\boxed{\begin{aligned} M_{\Xi(1690)} &= 1692.0 \pm 1.3^{+1.2}_{-0.4}\ \text{MeV} \\ \Gamma_{\Xi(1690)} &= 25.9 \pm 9.5^{+14.0}_{-13.5}\ \text{MeV} \end{aligned}}$$

$$M_{\Xi(1820)} = 1822.7 \pm 1.5^{+1.0}_{-0.6}\ \text{MeV}$$

$$\Gamma_{\Xi(1820)} = 36.0 \pm 4.4^{+7.8}_{-8.2}\ \text{MeV}$$

ΛK^- Correlation Function

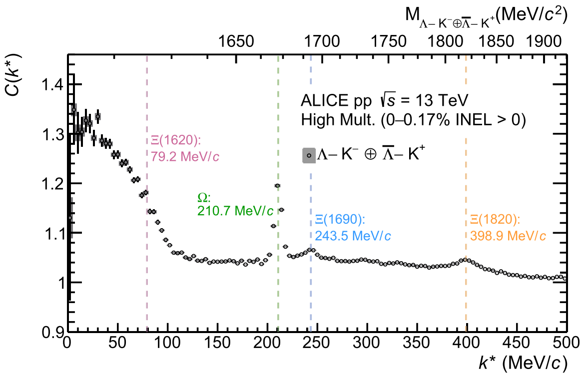

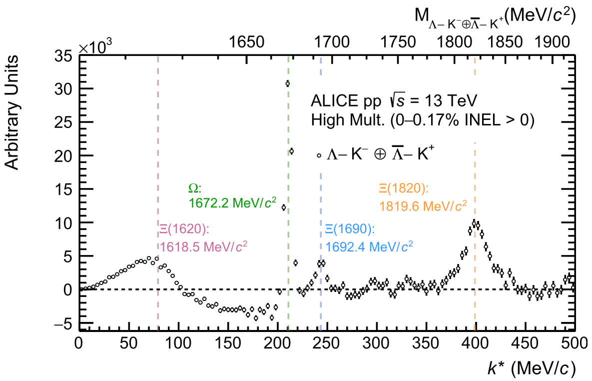

$$f(k^*) = \frac{-2\Gamma_{\Lambda K^-}}{E^2 - M^2 + i\Gamma_{\Xi\pi}\sqrt{E^2 - E^2_{thr.\Xi\pi}} + i\Gamma_{\Lambda K^-}\sqrt{E^2 - E^2_{thr.\Lambda K^-}}}$$

$\Xi(1620)$ properties obtained from a Flatté distribution in the analysis:

$$M = 1618.49 \pm 0.28\ (\text{stat}) \pm 0.21\ (\text{syst})\ \text{MeV}$$

$$\Gamma_{\Xi\pi} = 1.01 \pm 0.14\ (\text{stat}) \pm 0.39\ (\text{syst})\ \text{MeV}$$

$$\Gamma_{\Lambda K^-} = 115.99 \pm 8.56\ (\text{stat}) \pm 4.08\ (\text{syst})\ \text{MeV}$$

Compatibility study between $K^-\Lambda$ CF and $K^-\Lambda$ IMD from $\Xi_b^- \to J/\psi K^-\Lambda$

INSTITUT DE FÍSICA CORPUSCULAR

c) $J/\psi\Lambda$ FSI (HQSS and HG formalism) *A.F., W.F. Wang, C. W. Xiao et al., Phys.Lett.B* 839 (2023) 137760

- S=-1 and hidden charm Vector-baryon (1/2$^+$): $J/\psi\Lambda(4212.6), \bar{D}_s^*\Lambda_c(4398.7), \bar{D}^*\Xi_c(4477.6), \bar{D}^*\Xi_c'(4587.0)$

- Interaction consisting in a t-channel (mediated by a vector) reduced to a contact term (s-wave)

$V_{ij} = C_{ij}\frac{1}{4f_\pi^2}(p^0 + p'^0)$, used as input for the BS eq. to get a unitarized T-matrix from which we get:

Poles are degenerate in spin: $J^P = 1/2^-, 3/2^-$

VLC Model	$P_{cs}(4413)$	$P_{cs}(4570)$
M [MeV]	4413.18	4569.93
Γ [MeV]	12.80	8.32
	g_i	g_i
$J/\psi\Lambda$	$0.28 - i0.05$	$0.51 - i0.02$
$\bar{D}_s^*\Lambda_c$	$0.76 + i0.29$	$0.04 - i0.02$
$\bar{D}^*\Xi_c$	$2.99 + i0.15$	$-0.03 + i0.02$
$\bar{D}^*\Xi_c'$	$0.02 - i0.05$	$2.07 - i0.13$

→ In this theoretical paper, the LHCb $P_{\psi s}^N(4459)$ was associated to a state generated in the PB sector $(D'\Xi_c')$

→ The original $P_{cs}(4413)$ was in Good agreement with the observed $P_{\psi s}^N(4338)$, due to the change of regularization method shifted 75 MeV upward

→ In analogy with the P_ψ^N, a third pentaquark may still exist $P_{cs}(4570)$???

Motivation: Ξ(1620) and Ξ(1690) molecular nature

INSTITUT DE FÍSICA CORPUSCULAR

Taking the lowest order of the chiral lagrangian, exactly SU(3) invariant, one has

$$V_{ij} = C_{ij}\frac{1}{4f^2}(2\sqrt{s} - M_i - M_j)\left(\frac{M_i + E_i}{2M_i}\right)^{1/2}\left(\frac{M_j + E_j}{2M_j}\right)^{1/2}$$

All M_j=M (baryons)
All m_j=m (mesons)

In the SU(3), combining the ground-state baryon octet with the pseudoscalar one and decomposing into irreps

$$8 \otimes 8 = 1 \oplus 8_s \oplus 8_a \oplus 10 \oplus \overline{10} \oplus 27$$

In the SU(3) basis, the interaction should be diagonal with eigenvalues λ → the attractive eigenvalues allow the dynamical generation of bound states and resonances

$$\lambda_{\alpha\beta} = \sum_{i,j} \langle i|\alpha\rangle C_{ij} \langle j|\beta\rangle \rightarrow \lambda_{\alpha\beta} = diag(-6, -3, -3, 0, 0, 2)$$

- In S=-1 (I=0): 2 degenarate Λ^*'s generated from the 8_s and 8_a and a more bound Λ^* from the singlet (1) → (restablishing physical masses) → $\Lambda(1405)$ (2 poles from the singlet and one octet) and $\Lambda(1670)$ (from the other octet)

D. Jido et al, NPA 725 (2003) 181-200

- In S=-2 (I=1/2): 2 degenerate Ξ^*'s from 8_s and 8_a → expected $\Xi(1620)$ and $\Xi(1690)$